Check for updates

Received: 18 May 2025 | Accepted: 26 September 2025

DOI: 10.1111/1365-2435.70201

RESEARCH ARTICLE

Functional Ecology

Savanna tree species show contrasting acclimation responses to elevated atmospheric CO_2 concentration and drought

Edith J. Singini[1,2] | Sally Archibald[2] | Colin P. Osborne[3] | Brad S. Ripley[1]

[1]Botany Department, Rhodes University, Grahamstown, South Africa

[2]School of Animal, Plant and Environmental Sciences, University of the Witwatersrand, Johannesburg, South Africa

[3]Plants, Photosynthesis and Soil, School of Biosciences, University of Sheffield, Sheffield, UK

Correspondence
Edith J. Singini
Email: edith.singini@ru.ac.za

Funding information
National Research Foundation, Grant/Award Number: CPRR23030680939; Natural Environment Research Council, Grant/Award Number: NE/T000759/1

Handling Editor: Mark Tjoelker

Abstract

1. Woody plant expansion into historically grass-dominated savannas is reshaping ecosystem structure and function, with consequences for biodiversity, nutrient cycling and land use. This shift is thought to be driven by the physiological responses of certain C_3 tree species to elevated atmospheric CO_2 concentrations (eCO_2), modulated by water availability, among other constraints. However, the species-specific mechanisms regulating photosynthetic acclimation under these conditions remain unclear.
2. Using an Open-Top Chamber system, we examined the responses of five southern African C_3 tree seedlings to ambient (400 ppm) and elevated (550 ppm) CO_2 concentrations under contrasting soil water availability.
3. Our results revealed that *Vachellia karroo*, *V. tortilis* and *V. sieberiana* exhibited clear photosynthetic upregulation under eCO_2, with increased photosynthetic capacity (carboxylation capacity and/or electron transport rate), particularly under well-watered conditions when stomatal conductance was highest. These responses diminished under water limitation but remained higher than in *V. robusta* and *Senegalia burkei*, which downregulated under eCO_2 at high water availability and showed only modest improvements under dry conditions. Importantly, photosynthetic upregulation did not consistently translate into above-ground growth gains, with significant enhancement observed only in *V. sieberiana* under high water supply.
4. These divergent acclimation strategies highlight why some species emerge as dominant encroachers under rising CO_2, while others remain constrained by stronger physiological limitations.

KEYWORDS
climate change, gas exchange, photosynthetic acclimation, physiological resilience, woody plant encroachment

This is an open access article under the terms of the Creative Commons Attribution License, which permits use, distribution and reproduction in any medium, provided the original work is properly cited.
© 2025 The Author(s). *Functional Ecology* published by John Wiley & Sons Ltd on behalf of British Ecological Society.

1 | INTRODUCTION

Savannas are functionally defined as ecosystems where a continuous C_4 grass layer coexists with shade-intolerant trees (Ratnam et al., 2011). In most savannas, the herb layer is dominated by shade-intolerant C_4 grasses, whereas the woody layer consists predominantly of C_3 trees, producing a discontinuous/open tree canopy (Bond & Midgley, 2012; Scholes & Archer, 1997). The discontinuous tree cover is often attributed to bottlenecks that limit the establishment of tree seedlings and their recruitment into adult-size classes (Bond & Midgley, 2012; Higgins et al., 2000; Scholes & Archer, 1997). Global increases in tree cover have been observed within these ecosystems (Scholes & Archer, 1997; Skowno et al., 2017). One possible driver is elevated atmospheric CO_2 concentrations (eCO_2), promoting the competitive ability of C_3 trees and releasing the bottlenecks that limit tree recruitment (Bond & Midgley, 2000; Raubenheimer & Ripley, 2022; Stevens et al., 2017). These changes may have long-term consequences, altering ecosystem structure and function, impacting biodiversity richness, ecosystem services and wildlife populations (Bora et al., 2021; Criado et al., 2020).

While increases in woody encroachment have been widely observed across savanna ecosystems, they are not driven uniformly by all tree species (Stevens et al., 2017). For instance, while *Vachellia karroo* and *V. tortilis* are commonly identified as dominant encroachers in South African grasslands (O'Connor et al., 2014; Wigley et al., 2009), often forming dense thickets, other congeners such as *V. luederitzii*, which is widespread in arid savannas, are less frequently associated with woody encroachment (Kellner et al., 2022; Skowno et al., 2017). These species-level differences suggest that certain trees may be more physiologically responsive to environmental change than others, but the mechanisms behind this remain poorly understood. One proposed explanation is the differential acclimation of photosynthetic capacity under eCO_2, which influences how efficiently plants assimilate carbon and convert it into biomass. For instance, previous work on *V. karoo* has shown that it upregulates photosynthetic capacity in response to eCO_2 (Bellasio et al., 2021; Quirk et al., 2019; Raubenheimer & Ripley, 2022), that is, increases from the ambient-CO_2 baseline. This upregulation could explain its rapid growth rates, which contrasts with the common response of many tree species that downregulate photosynthesis under eCO_2 (Campany et al., 2017; Flexas et al., 2004; Ruiz-Vera et al., 2017).

Photosynthetic up- or downregulation can be determined by measuring the response of net leaf CO_2 assimilation (*A*) to intercellular CO_2 (Ci) concentrations (Farquhar & Sharkey, 1982; Flexas et al., 2004; Medrano et al., 2002). This method characterises key parameters, including the initial slope of the *A*Ci response, which defines the maximum rate of carboxylation by Rubisco, ribulose-1,5-bisphosphate carboxylase/oxygenase (*V*cmax) and the saturated slope, which determines the maximum rate of electron transport (*J*max). Increases in these parameters would indicate upregulation, while the converse would indicate downregulation. The actual prevailing photosynthetic rate, however, depends on Ci and whether photosynthesis is limited by *V*cmax and/or *J*max (Huxman et al., 1998; Vu et al., 2006; Zheng et al., 2019). When Ci is low, photosynthesis is typically limited by *V*cmax, while at higher Ci levels, it is constrained by *J*max. Therefore, understanding the limitations imposed by *V*cmax and *J*max helps to elucidate the regulatory mechanisms of photosynthesis under different environmental conditions.

Growth under eCO_2 often results in the downregulation of photosynthesis due to an imbalance between the production of non-structural carbohydrates and their export or utilisation in growth and respiration. This imbalance may be further constrained by nutrient availability, particularly when nitrogen or phosphorus is limiting (Campany et al., 2017; Kirschbaum, 2011; Zotz et al., 2005). The foliar accumulation of carbohydrates signals the repression of genes such as rbcS (the small subunit of Rubisco), leading to downregulation of photosynthesis and readjustment of the source–sink balance (Aranjuelo et al., 2005; Campany et al., 2017; Ruiz-Vera et al., 2017). Conversely, if sink strengths are adequate and not restricted by nutrient limitations, biochemical upregulation may occur, resulting in enhanced photosynthesis (Major et al., 2022; Ruiz-Vera et al., 2017). Over longer time-scales, however, CO_2 fertilisation effects may diminish due to progressive nutrient limitation (PNL), as accumulating biomass increasingly restricts nitrogen and phosphorus availability (Jiang et al., 2020; Luo et al., 2004). Thus, PNL is likely to regulate both the persistence and the magnitude of eCO_2 responses in savannas.

Changes in soil water availability can also drive upregulation or downregulation of photosynthesis (Bota et al., 2004; Medrano et al., 2002). When drought limits stomatal conductance and Ci, there are direct biochemical alterations to photosynthesis that can decrease both *V*cmax and *J*max (Flexas et al., 2004; Grassi & Magnani, 2005; Kohzuma et al., 2009; Medrano et al., 2002). However, under conditions of water availability, when stomatal conductance is high and when neither nutrients nor light limit photosynthesis, water-driven upregulation of photosynthesis can occur. This is characterised by an increase in leaf nitrogen as well as Rubisco and is associated with an overall increase in light harvesting and CO_2 assimilation capacity (Demmig-Adams et al., 2017).

Given the ecological consequences of woody expansion and the environmental changes driving it, there is a pressing need to understand the physiological mechanisms that enable certain tree species to respond more strongly to eCO_2 and variable water availability. In this study, we investigated the responses of five southern African C_3 tree species to ambient (400 ppm) and elevated (550 ppm) CO_2 concentrations under contrasting soil water conditions, using a controlled Open-Top Chamber system at the Rhodes University Elevated CO_2 Facility (RUECF). We hypothesised that savanna tree species would differ in their capacity for photosynthetic acclimation to eCO_2. In particular, we hypothesised that species previously observed to encroach (such as *V. karroo*, *V. sieberiana* and *V. tortilis*) would show stronger upregulation of photosynthetic capacity under eCO_2, reflected in increases in *V*cmax, *J*max and assimilation rate (*A*), particularly under well-watered conditions. Where sink capacity and water are sufficient, higher above-ground growth is expected, with growth advantages being species-dependent. In contrast, we expect that *V. robusta* and *Senegalia burkei*, which are not typically

13652435, 0, Downloaded from https://besjournals.onlinelibrary.wiley.com/doi/10.1111/1365-2435.70201 by UNIVERSITY OF SHEFFIELD, Wiley Online Library on [28/10/2025]. See the Terms and Conditions (https://onlinelibrary.wiley.com/terms-and-conditions) on Wiley Online Library for rules of use; OA articles are governed by the applicable Creative Commons License

associated with encroachment, would show limited or negative responses under eCO_2, possibly due to constraints in sink strength or resource allocation. We further anticipate that water limitation would suppress photosynthetic acclimation across all species, but that eCO_2 would partially alleviate drought-induced declines. Together, these patterns are expected to reveal species-specific physiological strategies linked to encroachment potential.

2 | MATERIALS AND METHODS

2.1 | Species selection

Five C_3 tree species from the subfamily Mimosoideae were selected based on their prevalence in southern African savannas and contrasting responses to environmental change (Figure S4). *V. karroo*, *V. tortilis* and *V. sieberiana* have frequently been identified as dominant encroachers across a range of savanna ecosystems, often forming dense thickets under eCO_2 or in response to land-use change (O'Connor et al., 2014; Stevens et al., 2017; Wigley et al., 2009). In contrast, *V. robusta* and *Senegalia burkei* are not typically associated with encroachment and are known to form sparse stands with slower growth or limited regeneration (Strauss & Packer, 2015; Rugemalila et al., 2017). Including these species allowed us to test whether physiological acclimation responses to CO_2 and water availability align with known ecological dynamics. Further ecological traits and encroachment evidence are detailed in Table S2. We focused on the seedling stage (within the first year of growth), since seedlings are particularly susceptible to environmental stress, and both survival and growth at this stage represent key demographic bottlenecks influencing population dynamics and community structure (Bond, 2008; Walters & Reich, 2000; Wigley et al., 2010). All species are indigenous to the region and are commonly found in savanna ecosystems.

2.2 | Experimental design and treatments

We used a split-plot factorial design to test the effects of atmospheric CO_2 and soil water availability on seedling performance. CO_2 concentration was applied at the chamber (whole-plot) level, while water availability was manipulated within chambers at the pot (subplot) level. Sixteen open-top chambers (OTCs; 3 m diameter, 2.8 m high; Ripley et al., 2022) were randomly assigned to either ambient CO_2 (aCO_2, 400 ppm; $n = 8$) or elevated CO_2 (eCO_2, 550 ppm; $n = 8$), with no positional bias (Table 1). Each chamber contained 30 pots (one seedling per pot, six individuals per species), which were randomly assigned to well-watered or dry treatments, yielding three individuals per species per water treatment per chamber. Across chambers, this provided up to 24 individuals per species per water treatment (Figure S1). For physiological and growth measurements, we analysed a random subset of 10 individuals per species per $CO_2 \times$ water combination (Table 1).

Seedlings were grown in 4 L cylindrical pots (diameter ~11.3 cm, height ~40 cm) filled with homogenised savanna soil. Seeds were germinated in September 2021 in vermiculite and were transplanted in November of the same year. Pots were placed near the centre of each OTC to minimise edge effects such as shading and localised warming (Figure S1). Seedling assignment to pots and chambers was fully randomised at transplanting to avoid treatment bias and ensure even representation across the design.

Atmospheric CO_2 within each OTC was continuously monitored with open-path infrared CO_2 sensors (GMP343, Vaisala, Finland). Concentrations were regulated by a proportional-integral-derivative (PID) controller and proportional valves (2873, Bürkert, Germany), with uniform air distribution maintained via a perforated diffuser connected to a canopy-level fan (Ripley et al., 2022). Daytime concentrations averaged 398 ppm (central 90%: 383–411 ppm) in aCO_2 chambers and 545 ppm (central 90%: 496–588 ppm) in eCO_2 chambers, representing ~150 ppm enrichment consistent with mid-21st century projections (IPCC, 2021).

Water availability was manipulated at the pot level. Well-watered plants were maintained near field capacity through daily irrigation, while dry treatment plants received no routine irrigation. To prevent mortality during prolonged droughts, minimal watering was applied when severe wilting occurred. Treatments commenced in January 2022, once seedlings were fully established. Episodic rainfall, during the sampling period, contributed additional inputs producing a continuum of soil moisture across pots despite the nominal dry versus well-watered assignments

TABLE 1 Summary of experimental replication and treatment application scales.

Scale of inference	Scale at which the factor of interest was applied	Number of replicates at the appropriate scale
Species (physiological and growth traits)	Pot (individual seedling)	6 per species per chamber (30 pots per chamber)
Treatment effect ($CO_2 \times$ water)	Chamber (CO_2) + pot within chamber (water)	16 chambers (8 aCO_2, 8 eCO_2); within each chamber, 3 pots per species per water treatment
Per combination availability	Across chambers at a given CO_2	Up to 24 individuals per species per water treatment; $n = 10$ used for analyses

13652435, 0, Downloaded from https://besjournals.onlinelibrary.wiley.com/doi/10.1111/1365-2435.70201 by UNIVERSITY OF SHEFFIELD, Wiley Online Library on [28/10/2025]. See the Terms and Conditions (https://onlinelibrary.wiley.com/terms-and-conditions) on Wiley Online Library for rules of use; OA articles are governed by the applicable Creative Commons License

(Figure S2). Over 12 months, rainfall totalled 301 mm, below the site's long-term mean (~466 mm; CHIRPS). Because rainfall affected all chambers equally, it was not included as a model covariate; its effects were instead captured by volumetric water content (VWC) measurements.

Microclimate was characterised using HygroVUE 5 sensors (Campbell Scientific) recording air temperature and relative humidity at 10-min intervals, allowing calculation of vapour pressure deficit (VPD). Soil moisture was monitored using 5TM sensors (METER Group, formerly Decagon), installed in four randomly selected pots per chamber (two per water treatment) and logged every 10 min. For leaf gas exchange, we matched each measurement to the instantaneous, treatment-level VWC from the relevant chamber. For growth analyses, we used the time-weighted mean VWC for each plant from transplanting to harvest. Within chambers, sensor values were averaged per water treatment, providing one VWC time series for each chamber × treatment combination (16 time series per treatment across the experiment; Figure S2).

2.3 | Measurements

Physiological responses were measured from 20 September to 17 October 2022, approximately 10 months after transplanting. The measurements were conducted using a block-randomised daily schedule that alternated chambers and water treatments across species, ensuring balanced sampling across dates and times (9:00 AM–3:00 PM). For a subset of plants from each species and treatment combination ($n > 8$ per species per treatment), we measured *A*Ci response curves (net CO_2 assimilation rate, *A*, vs. intercellular CO_2 concentration, Ci), stomatal conductance (g_{ST}) and above-ground growth rates. Physiological measurements were conducted using a portable photosynthesis system (LI-6800; LI-COR Biosciences, Lincoln, NE, USA) equipped with an environmental control module. *A*Ci curves were recorded across a range of soil volumetric water content (VWC; 3%–40%) to reflect conditions imposed by the experimental treatments. We analysed physiological responses against continuous VWC (instantaneous at the time of measurement). The plotted *A*Ci curves were binned into droughted (0%–10% VWC) and well-watered (15%–30% VWC) classes; curves falling in the intermediate 10%–15% range were not included in the binned panels. Because not every plant measurement fell within those bins, the binned *A*Ci had $n \geq 5$ but <8 per species per CO_2 level, whereas continuous VWC analyses used $n > 8$ per species per CO_2 level.

Photosynthetic parameters were computed using the automated *A*Ci response curve program in the LI-COR 6800 system. This CO_2 response protocol sequentially adjusted CO_2 concentrations while automatically logging data only after matching conditions were met, ensuring steady-state assimilation and stomatal conductance values at each point. This automated approach reduces observer bias, ensures consistent stabilisation criteria across all measurements and improves the precision of curve fitting. The standard CO_2 concentration sequence was 400, 300, 200, 100, 50, 400, 600, 800, 1000 and 1200 ppm for ambient-grown plants, with 550 ppm used instead of 400 ppm for eCO_2-grown plants. The selected CO_2 range captured both the Rubisco-limited and RuBP-limited portions of the photosynthetic response. The CO_2 concentration sequence used for *A*Ci curves reached a maximum of 1200 ppm, which was sufficient to observe saturation of net assimilation across all species. Fully expanded, healthy leaves were selected to fully cover the cuvette area and measurements were performed under standardised cuvette conditions: PPFD = 1500 μmol m^{-2} s^{-1}, leaf temperature = 25°C, fan speed 10,000 rpm and VPD < 1.6 kPa. Leaf area was quantified using scaled digital images processed in ImageJ (Fiji version 2016).

Curve fitting and parameter estimation were conducted in R using the 'plantecophys' package (Duursma, 2015), which implements the Farquhar–von Caemmerer–Berry photosynthesis model. From each fitted curve, *V*cmax and *J*max were extracted. We did not estimate mesophyll conductance (g_m); that is, we used Ci-based fits (Cc = Ci). The CO_2 compensation point in the absence of dark respiration (Γ^*), the Michaelis–Menten constants for Rubisco (K_c, K_o) and their temperature dependencies were held constant, calculated from leaf temperature using standard parameterisations implemented in 'plantecophys'. Photorespiratory O_2 was set to 21 kPa, and leaf temperature was controlled at 25°C during measurements. For each Ci value, the corresponding net assimilation rate was calculated as the minimum of Rubisco-limited (A_k) and RuBP-limited (A_j) photosynthesis. Mean predicted rates and standard deviations were computed across Ci values to summarise each plant's photosynthetic response profile.

We classified species' responses under well-watered conditions (15–30% VWC) as follows. 'Upregulation' was assigned when eCO_2 produced (i) a significant positive effect on *J*max and/or *V*cmax in mixed-effects models (CO_2 main effect > 0 at $p < 0.05$, or a positive $CO_2 \times$ VWC interaction with a positive simple effect at 20% VWC), and (ii) an upward shift in photosynthesis at growth CO_2 supported by model estimates/post-hoc contrasts. 'Limited/no upregulation' indicates criteria were not met, and 'downregulation' indicates significant negative parameter shifts with lower photosynthesis at eCO_2 and high VWC.

After completing the physiological measurements, plants were harvested in November 2022 ($n = 10$ for each treatment). The destructive harvest involved carefully cutting all above-ground leaves, stems and branches from each plant. To determine the dry biomass, the collected plant material was dried in a convection oven at a constant temperature of 70°C for a minimum of 72 h (3 days), or until the samples reached a constant weight. The samples were then weighed using a precision balance to the nearest 0.01 g. The growth rate of each plant was calculated by dividing the total above-ground dry biomass by the time elapsed from transplanting into pots in the OTC to the harvest date. We then quantified the above-ground growth rate as dry above-ground biomass accrued per unit time.

13652435, 0, Downloaded from https://besjournals.onlinelibrary.wiley.com/doi/10.1111/1365-2435.70201 by UNIVERSITY OF SHEFFIELD, Wiley Online Library on [28/10/2025]. See the Terms and Conditions (https://onlinelibrary.wiley.com/terms-and-conditions) on Wiley Online Library for rules of use; OA articles are governed by the applicable Creative Commons License

2.4 | Data analysis

All statistical analyses were conducted in R version 4.4.2 (R Core Team, 2024). Prior to formal analysis, all response variables were assessed for normality and homoscedasticity using Q–Q plots and residual-versus-fitted value plots. Where necessary, variables such as stomatal conductance and growth rate were log-transformed to improve model fit and stabilise variance.

To examine the effects of CO_2 concentration and soil water availability on physiological and growth responses, linear mixed-effects models were fitted using the 'lme4' package (Bates et al., 2015). In the first set of models, CO_2 treatment (ambient vs elevated), continuous VWC and species were included as fixed effects with their two- and three-way interactions ($CO_2 \times$ VWC $\times$ species; Supporting Information S1). Chamber number and date were included as random effects to account for shared environmental conditions experienced by plants within the same open-top chamber on different dates (Supporting Information S1). These models were run separately for each response variable: net photosynthetic rate, stomatal conductance, intercellular CO_2, *V*cmax, *J*max and above-ground growth rate. This approach enabled us to assess whether species responded differently to CO_2 and VWC. To present species-specific responses at each growth CO_2, we evaluated simple effects by fitting the same model within each CO_2 level (equivalent to probing the $CO_2 \times$ VWC $\times$ species interaction at aCO_2 and eCO_2). This allowed for a focused comparison of species performance under consistent CO_2 conditions, while still accounting for the nested chamber design. Type II *F*-tests were used for hypothesis testing via the ANOVA function in the 'car' package (Fox & Weisberg, 2019), which provides robust tests of marginal effects in unbalanced designs. When significant main or interaction effects were identified, post hoc pairwise comparisons were performed using the 'emmeans' package (Lenth, 2020), with Tukey's HSD correction for multiple comparisons. All statistical outputs were interpreted with attention to effect sizes and 95% confidence intervals.

3 | RESULTS

The tree species were sampled across VWC conditions ranging from 3% to 40% (Figure S2). In the watered treatment, VWC consistently remained above 15%, whereas the droughted treatment mainly experienced VWC levels between 3% and 10%, with the occasional increase of up to 15% due to infrequent and stochastic rainfall events (Figure S2).

When grown at aCO_2, *V. sieberiana*, *V. tortilis* and *V. karroo* had significantly higher photosynthetic rates (22.9, 22.4 and 21.9 $\mu mol\, m^{-2} s^{-1}$, respectively) than *V. robusta* (16.3 $\mu mol\, m^{-2} s^{-1}$) and *S. burkei* (15.3 $\mu mol\, m^{-2} s^{-1}$; $F_{(1,58.73)} = 350.15$, $p < 0.001$; Figures 1 and 2). As VWC decreased from 40% to 3%, the photosynthetic rate of all five species decreased, and there was a downward shift in the *A*Ci curves (Figures 1 and 2). The slope of the response to VWC was similar across species ($F_{(4,57.85)} = 0.59$, $p = 0.67$), indicating that for any given VWC level, *V. sieberiana*, *V. tortilis* and *V. karroo* consistently maintained higher photosynthetic rates than *V. robusta* and *S. burkei* ($F_{(4,58.57)} = 28.25$, $p < 0.001$).

The effect of eCO_2 on photosynthesis showed different responses for all five species ($F_{(4,33.96)} = 109.21$, $p < 0.001$) and depended

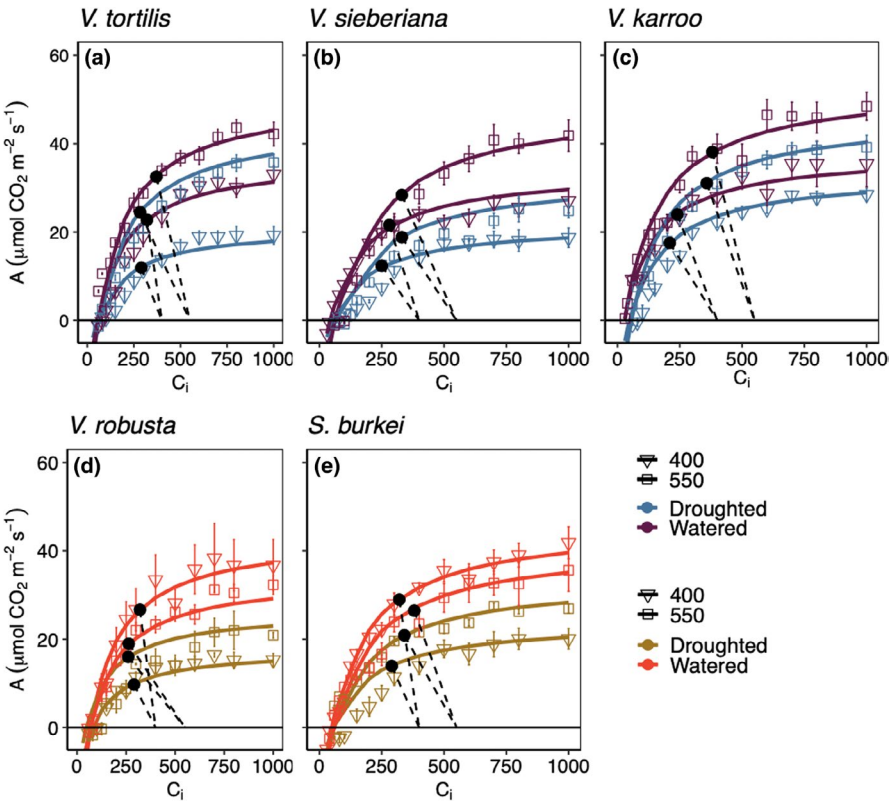

FIGURE 1 Observed *A*Ci data (mean ± SE) overlaid with fitted Farquhar-model curves for five savanna tree (*Vachellia karroo*, *V. robusta*, *V. tortilis*, *V. sieberiana* and *S. burkei*) seedlings exposed to differing CO_2 concentrations and water treatments, showing stomatal limitations (dotted lines). Stomatal limitation at growth CO_2 was computed for each curve as the difference between assimilation at the growth intercellular CO_2 (Ci) and assimilation at the growth atmospheric CO_2 (Ca). The top row panels represent species showing photosynthetic upregulation under eCO_2 and watered conditions, while the bottom panels denote species with limited or downregulation.

13652435, 0, Downloaded from https://besjournals.onlinelibrary.wiley.com/doi/10.1111/1365-2435.70201 by UNIVERSITY OF SHEFFIELD, Wiley Online Library on [28/10/2025]. See the Terms and Conditions (https://onlinelibrary.wiley.com/terms-and-conditions) on Wiley Online Library for rules of use; OA articles are governed by the applicable Creative Commons License

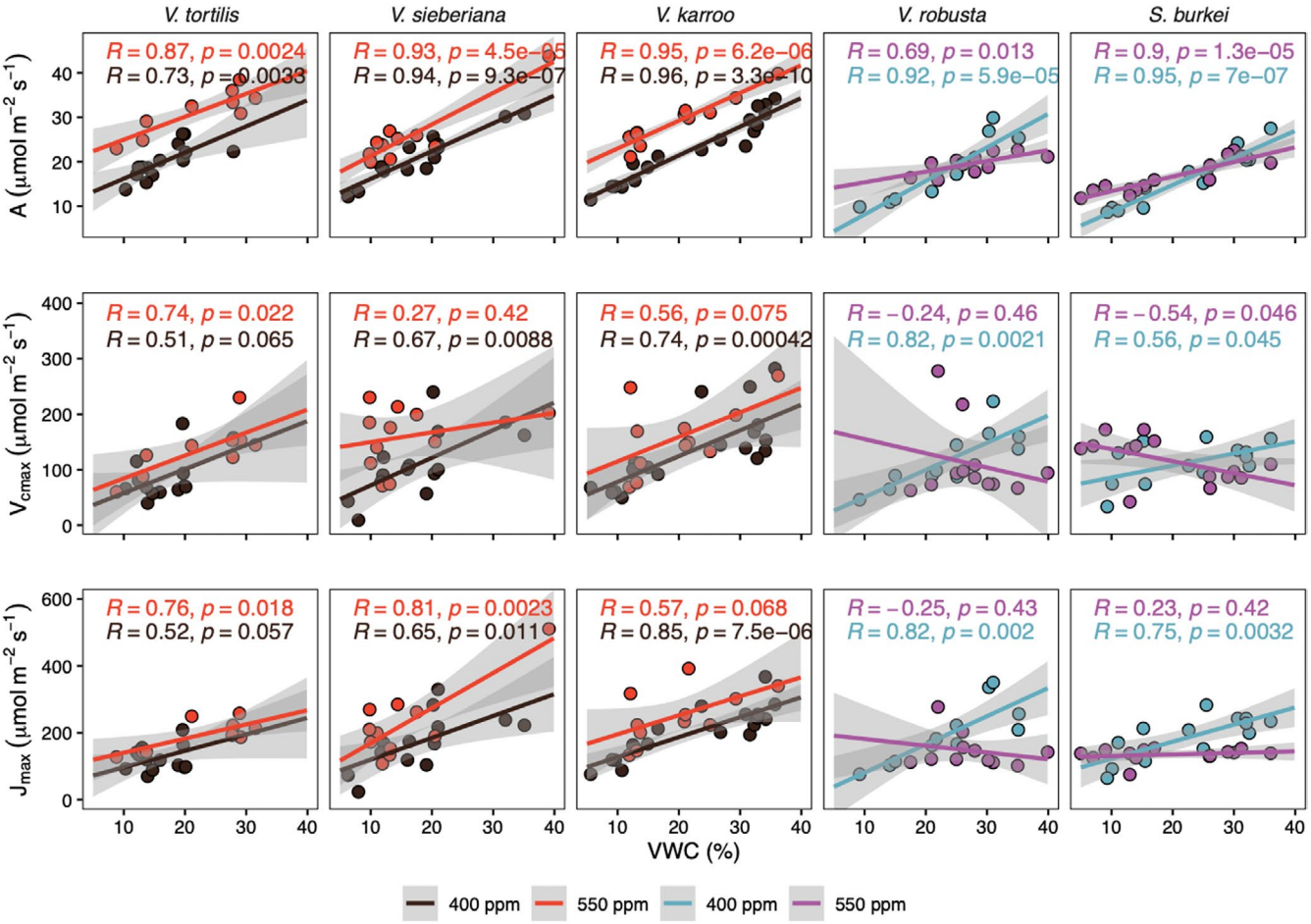

FIGURE 2 Linear regressions of five savanna tree seedlings (*Vachellia karroo*, *V. robusta*, *V. tortilis*, *V. sieberiana* and *S. burkei*) showing the net photosynthesis rate (*A* at growth CO_2), maximum carboxylation rate (*V*cmax) and maximum electron transport rate (*J*max) across volumetric soil water content (VWC) at 400 and 550 ppm. *A* at growth CO_2 is the measured assimilation recorded during the *A*Ci protocol at the plant's prevailing growth CO_2 under saturating light. Orange and brown points and lines represent species showing photosynthetic upregulation under eCO_2 and watered conditions, while blue and purple lines denote species with limited or downregulation.

on soil water availability ($F_{(4,37.11)}=5.72$, $p<0.01$; Figure 2). Under high VWC, eCO_2 led to higher photosynthetic rates in *V. sieberiana*, *V. tortilis* and *V. karroo* but lower photosynthetic rates in *V. robusta* and *S. burkei* ($F_{(4,33.96)}=109.21$, $p<0.001$), that is, well-watered *V. sieberiana*, *V. tortilis* and *V. karroo* showed an upward shift in the *A*Ci curve at eCO_2 while well-watered *V. robusta* and *S. burkei* showed a downward shift in the *A*Ci curve (Figure 1). As VWC decreased, photosynthesis also decreased across all species. However, under extremely dry conditions (<10% VWC), all the five species benefitted from eCO_2 and were able to maintain higher photosynthetic rates than at ambient levels (Figure 2). Therefore, at eCO_2, *V. sieberiana*, *V. tortilis* and *V. karroo* exhibited upregulation across varying soil water conditions which alleviated the constraints of drought, but *V. robusta* and *S. burkei* only benefited from eCO_2 when drought-stressed, and downregulated at high CO_2 and high VWC (Figure 1). Overall, eCO_2 enabled *V. sieberiana*, *V. tortilis* and *V. karroo* to mitigate the effects of decreasing VWC more than *V. robusta* and *S. burkei*.

*V*cmax showed distinct responses to VWC and CO_2 levels across species (Figure 2). In *V. karroo*, *V*cmax increased significantly with VWC ($F_{(1,23.0)}=19.19$, $p<0.001$), while eCO_2 and the interaction term were not significant ($p>0.17$; Table S1). In *V. sieberiana*, both VWC ($F_{(1,20.54)}=6.54$, $p=0.019$; Figure 2) and CO_2 ($F_{(1,8.81)}=6.06$, $p=0.037$) had significant effects on *V*cmax, whereas the interaction was not significant ($p=0.23$; Table S1). *V. tortilis* also exhibited a significant increase in *V*cmax with VWC ($F_{(1,11.94)}=10.76$, $p=0.007$; Figure 2), but not in response to CO_2 or the interaction ($p>0.25$; Table S2). In contrast, *S. burkei* and *V. robusta* showed significant VWC × CO_2 interactions ($p<0.05$; Table S1), with no main effects. In these species, *V*cmax declined under eCO_2 at high VWC. Thus, *V*cmax responses aligned with the direction of *A*Ci curve shifts observed across species.

*J*max showed similar differences among species (Figure 2). In *V. karroo*, *J*max increased significantly with VWC ($F_{(1,24.98)}=28.12$, $p<0.001$) and also with eCO_2 ($F_{(1,5.22)}=7.67$, $p=0.038$) but with no interaction. *V. sieberiana* exhibited the same pattern; both VWC ($F_{(1,20.54)}=23.66$, $p<0.001$) and CO_2 ($F_{(1,8.81)}=6.48$, $p=0.032$) had significant effects, with no interaction ($p>0.05$; Table S1). In *V. tortilis*, *J*max also increased significantly with VWC ($F_{(1,11.94)}=10.89$,

13652435, 0, Downloaded from https://besjournals.onlinelibrary.wiley.com/doi/10.1111/1365-2435.70201 by UNIVERSITY OF SHEFFIELD, Wiley Online Library on [28/10/2025]. See the Terms and Conditions (https://onlinelibrary.wiley.com/terms-and-conditions) on Wiley Online Library for rules of use; OA articles are governed by the applicable Creative Commons License

$p = 0.006$), although neither CO_2 nor the interaction was significant ($p > 0.05$; Table S1). In *S. burkei* and *V. robusta*, all terms were significant ($p < 0.05$), with both species showing *J*max decline under eCO_2 at high VWC but increased at low VWC. These results demonstrate that *J*max was positively regulated by VWC and CO_2 in *V. karroo*, *V. sieberiana* and *V. tortilis*, while photosynthetic upregulation in *S. burkei* and *V. robusta* was more constrained due to a strong interaction between water and CO_2 concentrations.

Stomatal conductance (g_{ST}) also exhibited distinct species-specific responses to VWC and atmospheric CO_2 concentration (Figure 3). In *V. karroo*, g_{ST} increased significantly with rising VWC ($F_{(1,24.98)} = 11.43$, $p = 0.002$), while CO_2 and the interaction term had no significant effects ($p > 0.4$; Table S1). In *V. sieberiana*, neither VWC ($F_{(1,17.54)} = 0.34$, $p = 0.57$), CO_2 ($F_{(1,11.71)} = 3.56$, $p = 0.084$) nor their interaction ($F_{(1,17.81)} = 0.32$, $p = 0.58$) was statistically significant, although a trend of reduced g_{ST} under eCO_2 was noted. In *V. tortilis*, none of the terms were significant; however, g_{ST} tended to be lower at eCO_2 ($F_{(1,3.93)} = 6.37$, $p = 0.066$; Table S1), suggesting a potential CO_2 sensitivity. In *S. burkei*, g_{ST} increased significantly with VWC ($F_{(1,19.18)} = 8.13$, $p = 0.01$), while CO_2 and the interaction were not significant ($p > 0.05$; Figure 3). Similarly, in *V. robusta*, g_{ST} was unaffected by either VWC, CO_2 or their interaction ($p > 0.1$; Table S1). These results suggested that water availability was the primary determinant of g_{ST} in *V. karroo* and *S. burkei*, while eCO_2 exerted a more uniform, but often non-significant, suppressive effect across all species.

Intercellular CO_2 concentration (Ci) patterns were consistent with *A*Ci curve trends (Figure 3). In *V. tortilis*, Ci increased significantly under eCO_2 and high VWC ($F_{(1,4.11)} = 25.44$, $p = 0.007$), while in *S. burkei*, a significant VWC effect ($F_{(1,22.79)} = 10.60$, $p = 0.004$) and a marginally significant interaction ($F_{(1,22.94)} = 3.05$, $p = 0.094$; Figure 3) were evident. On the contrary, Ci did not change significantly in

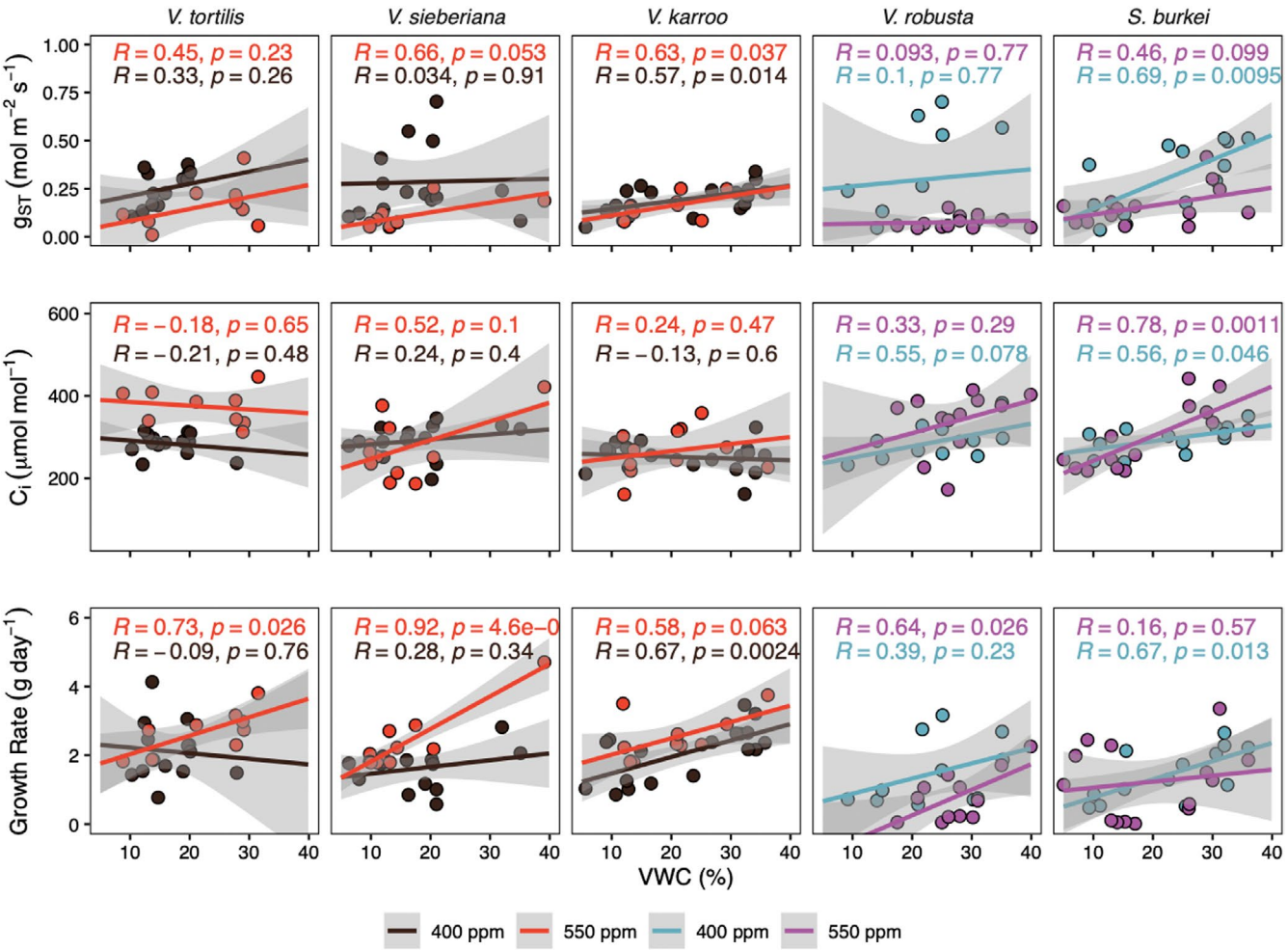

FIGURE 3 Linear regressions of five savanna tree seedlings (*Vachellia karroo*, *V. robusta*, *V. tortilis*, *V. sieberiana* and *S. burkei*) showing stomatal conductance (g_{ST}), intercellular CO_2 concentration (Ci) and above-ground growth rate versus volumetric water content (VWC) at CO_2 concentrations of 400 and 550 ppm. g_{ST} values were extracted from the *A*Ci response curves measured at the plant's respective growth CO_2 concentration (either 400 or 550 ppm) under saturating light. Growth rate (above-ground biomass gain per unit time) is related to each plant's mean VWC (time-averaged chamber-treatment VWC from transplanting to harvest). Orange and brown points and lines represent species showing photosynthetic upregulation under eCO_2 and watered conditions, while blue and purple lines denote species with limited or downregulation.

13652435, 0, Downloaded from https://besjournals.onlinelibrary.wiley.com/doi/10.1111/1365-2435.70201 by UNIVERSITY OF SHEFFIELD, Wiley Online Library on [28/10/2025]. See the Terms and Conditions (https://onlinelibrary.wiley.com/terms-and-conditions) on Wiley Online Library for rules of use; OA articles are governed by the applicable Creative Commons License

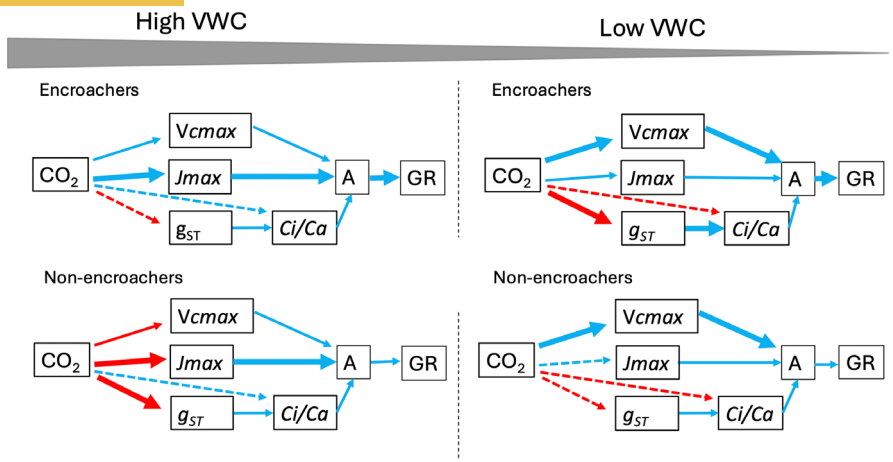

FIGURE 4 Conceptual summary of observed physiological responses illustrating the influence of atmospheric CO_2 concentration (400 and 550 ppm) and soil water availability (high vs low VWC) on key photosynthetic parameters (maximum carboxylation rate of Rubisco—*V*cmax, maximum electron transport rate—*J*max, stomatal conductance—g_{ST} and intercellular CO_2 concentration relative to ambient—Ci/Ca), as well as photosynthetic rate (*A*) and growth rate (GR), in encroaching and non-encroaching savanna tree species. The model is derived from observed statistical trends across species in the experimental dataset (see Table S1). Blue arrows indicate positive effects, red arrows indicate negative effects and dashed arrows represent a non-significant effect. Arrow thickness denotes the relative magnitude of the response.

response to VWC, CO_2, or their interaction ($p > 0.32$; Table S1) in *V. karroo*, *V. sieberiana* and *V. robusta*. These results indicated that biochemical capacity rather than CO_2 diffusion was the primary constraint on photosynthesis in most species (Figure S3). However, where Ci increased under eCO_2, as in *V. tortilis*, the observed photosynthetic enhancement was likely driven by improved internal CO_2 availability.

Above-ground growth responses only partially reflected physiological patterns (Figure 3). In *V. karroo*, the growth rate increased significantly with rising VWC ($F_{(1,24.98)} = 15.21$, $p < 0.001$), with a marginally positive CO_2 effect ($F_{(1,5.22)} = 4.34$, $p = 0.089$) and no interaction (Table S1). *V. sieberiana* showed significant effects of VWC ($F_{(1,20.57)} = 18.13$, $p < 0.001$), CO_2 ($F_{(1,10.44)} = 14.29$, $p < 0.01$) and their interaction ($F_{(1,20.40)} = 8.70$, $p < 0.01$). Although the CO_2 main effect was negative (Table S1), the positive interaction indicates that eCO_2 enhanced growth under high water availability, consistent with the increased photosynthetic capacity under these conditions. *V. tortilis* showed no significant effects, although small increases at eCO_2 were observed ($p > 0.05$; Figure 3; Table S1). *S. burkei* did not exhibit significant responses to any factor, and *V. robusta* showed a marginal effect of VWC ($F_{(1,15.92)} = 4.38$, $p = 0.053$) and a significant reduction in growth at eCO_2 ($F_{(1,8.74)} = 6.76$, $p = 0.03$; Table S1). Although above-ground growth rates generally increased with rising VWC in *V. karroo* and *V. sieberiana*, only *V. sieberiana* exhibited a significant above-ground growth response to eCO_2 and only under high water availability. In the other species, enhanced photosynthetic capacity under eCO_2 did not consistently translate into increased above-ground growth.

To integrate the observed physiological and growth patterns, we present a summary diagram (Figure 4) derived from model estimates and binned *A*Ci responses (Table S1; Figures 1–3). The figure compiles, for each species group, the direction and relative magnitude of responses in A, *V*cmax, *J*max, g_{ST}, Ci/Ca and above-ground growth under aCO_2 and eCO_2 at high and low VWC. Encroaching species (*V. karroo*, *V. sieberiana* and *V. tortilis*) are shown with the set of parameter shifts observed in Figures 1–3, and non-encroaching species (*V. robusta* and *S. burkei*) with their corresponding shifts; arrow thickness and sign reflect the estimated effect sizes and directions reported in Table S1.

4 | DISCUSSION

Using a comparison of five widespread southern African C_3 savanna tree species, we assessed the effects of anticipated future CO_2 levels and water availability on seedling performance. Our findings revealed distinct species-level differences in photosynthetic acclimation and growth, pointing to divergent strategies that may underpin shifts in savanna composition and function as atmospheric CO_2 concentrations and rainfall regimes change. As hypothesised, under current aCO_2 conditions and adequate water availability, *V. sieberiana*, *V. tortilis* and *V. karroo* exhibited higher net photosynthetic and growth rates compared to *V. robusta* and *S. burkei*. These differences were underpinned by higher values of *V*cmax and/or *J*max, despite relatively similar intercellular CO_2 concentrations, indicating that *V. sieberiana*, *V. tortilis* and *V. karroo* possess greater intrinsic biochemical capacity for carbon fixation. As water availability declined, photosynthetic rates decreased in all species; however, *V. sieberiana*, *V. tortilis* and *V. karroo* maintained relatively higher assimilation rates across the soil water gradient. Their ability to sustain high *V*cmax and/or *J*max values under drought points to greater physiological resilience, likely contributing to their broader distribution in both mesic and semi-arid regions (Bellasio et al., 2021; Buitenwerf et al., 2012; Telford et al., 2023).

13652435, 0, Downloaded from https://besjournals.onlinelibrary.wiley.com/doi/10.1111/1365-2435.70201 by UNIVERSITY OF SHEFFIELD, Wiley Online Library on [28/10/2025]. See the Terms and Conditions (https://onlinelibrary.wiley.com/terms-and-conditions) on Wiley Online Library for rules of use; OA articles are governed by the applicable Creative Commons License

These species also showed strong responses to eCO_2, particularly under well-watered conditions. *V. sieberiana* significantly increased *J*max and *V*cmax under eCO_2, with corresponding increases in photosynthesis and growth. In *V. karroo*, upregulation under eCO_2 manifested via increased *J*max (not *V*cmax) and higher photosynthesis at growth CO_2 under high VWC, consistent with an electron-transport-driven response. *V. tortilis* also benefited from eCO_2, albeit to a lesser degree (Figure 2). Their enhanced performance across both high and low VWC conditions suggests that these species may be particularly well positioned to thrive in future savannas subject to rising CO_2 and episodic water availability.

In contrast, *S. burkei* and *V. robusta* showed limited or negative responses to eCO_2 under high water availability, with declines in both *V*cmax and *J*max indicative of photosynthetic downregulation (Figures 1 and 2). This likely reflects source–sink imbalances, where assimilated carbon is not effectively utilised or exported (Campany et al., 2017; Sala et al., 2012). Interestingly, under drought, these same species exhibited modest improvements in photosynthesis at eCO_2, suggesting that increased CO_2 may partially alleviate diffusional limitations under stress (Flexas et al., 2004). However, this drought-associated response was not sufficient to overcome their generally lower physiological plasticity and constrained growth, particularly in well-watered conditions.

While eCO_2 increased leaf-level photosynthesis and capacities (*V*cmax, *J*max) in several species, this did not consistently translate into higher above-ground growth across species or moisture levels (Figure 3). This decoupling between photosynthesis and above-ground RGR at the seedling stage is consistent with shifts in carbon allocation and utilisation: additional assimilate under eCO_2 can be directed below-ground (roots/rhizosphere) (Case et al., 2020; Jiang et al., 2020; Lewis et al., 2021; McDowell et al., 2008), stored as non-structural carbohydrates (Jiang et al., 2020; Li et al., 2018; Sala et al., 2012) or offset by higher respiration (Drake et al., 2011), particularly when water or nutrients constrain structural shoot growth. Below-ground allocation may also enhance associations with soil mutualists such as mycorrhizas and rhizobia, which increase nutrient acquisition and can strengthen sink demand (Case et al., 2020; Jiang et al., 2020). Because our growth metric is above-ground only, such re-partitioning would reduce apparent RGR gains even when photosynthesis increases. Consequently, we interpret the eCO_2 benefit as physiological potential that translates into growth conditionally, most clearly in *V. sieberiana* at high VWC, rather than a general growth advantage among encroaching species.

While our approach focused on species-level responses, the emerging physiological patterns also lend support to a functional distinction between potential encroachers and non-encroachers (Figure 4). *V. karroo*, *V. sieberiana* and *V. tortilis* exhibited the traits of encroaching species: sustained photosynthetic capacity across water gradients, responsiveness to eCO_2, and robust growth performance (Raubenheimer & Ripley, 2022; Telford et al., 2023). These species are also well-documented encroachers in both empirical field studies and meta-analyses (Table S2), and their geographical spread across African savannas (Figure S4) reflects their ecological competitiveness. In contrast, *S. burkei* and *V. robusta* exhibited limited plasticity, greater sensitivity to high CO_2 levels and constrained growth, aligning with traits of non-encroachers (Rugemalila et al., 2017). These divergent responses may not only reflect differences in acclimation capacity but could also be rooted in underlying ecological preferences or phylogenetic constraints. For instance, *V. robusta* is often associated with riparian habitats (Rugemalila et al., 2017), which may predispose it to narrower physiological tolerance ranges. Meanwhile, *S. burkei*, which belongs to a different genus than the other study species (Kyalangalilwa et al., 2013), may exhibit distinct trait syndromes that limit its responsiveness to eCO_2 and water stress.

Together with the synthesis provided in Figure 4, these findings highlight how encroaching species consistently exhibit greater acclimation potential under rising CO_2 and variable water conditions, reinforcing their capacity to dominate under future climate scenarios. This framework suggests that species-level differences in acclimation potential may explain observed encroachment trends in empirical datasets and highlights the importance of incorporating species traits into ecosystem modelling (Figure 4). As atmospheric CO_2 continues to rise, species such as *V. sieberiana* may gain a further competitive edge, not only through increased photosynthesis and growth but by reaching fire-escape thresholds more rapidly and establishing dominance in both mesic and arid savanna systems. This aligns with projections from dynamic vegetation models, which predict that eCO_2 will favour tree recruitment in savannas (Higgins & Scheiter, 2012; Scheiter & Higgins, 2009). These shifts, although driven by only a few woody species with the physiological capacity to respond to CO_2, could result in the gradual replacement of open-canopy savannas by more densely wooded systems, ultimately reducing grass layer cover and altering fire regimes, herbivore dynamics and ecosystem services (Bond & Midgley, 2000; Staver et al., 2011).

Finally, while our study captures the key physiological mechanisms underlying species-specific responses to eCO_2 and variable soil water availability, it is important to recognise that broader ecosystem outcomes will be shaped by multiple interacting factors. These include nutrient availability, plant–microbe associations, disturbance regimes and interspecific competition, all of which may further modulate photosynthetic acclimation and growth (Bora et al., 2021; Sala et al., 2012). As such, predicting the precise consequences of CO_2 enrichment for savanna vegetation requires comprehensive, long-term research and models that integrate these complex relationships.

By offering species-level insights into the mechanisms that drive photosynthetic upregulation and growth under future CO_2 and water regimes, this study contributes to a growing body of evidence calling for greater functional resolution in vegetation models. The clear divergence in response among co-occurring species highlights the limitations of grouping trees into broad functional types without accounting for underlying physiological variation. Incorporating these encroacher versus non-encroacher traits into global models

13652435, 0, Downloaded from https://besjournals.onlinelibrary.wiley.com/doi/10.1111/1365-2435.70201 by UNIVERSITY OF SHEFFIELD, Wiley Online Library on [28/10/2025]. See the Terms and Conditions (https://onlinelibrary.wiley.com/terms-and-conditions) on Wiley Online Library for rules of use; OA articles are governed by the applicable Creative Commons License

will improve our ability to forecast savanna dynamics and develop adaptive strategies for conservation and land management in a rapidly changing climate.

AUTHOR CONTRIBUTIONS

Edith J. Singini collected and analysed data and led the writing of the manuscript. Brad S. Ripley conceived, designed and contributed to manuscript editing. Sally Archibald supervised the research and provided critical revisions to the manuscript. Colin P. Osborne funded the study, contributed to the study design and provided substantial input during the manuscript review process.

ACKNOWLEDGEMENTS

The research was supported by the Natural Environment Research Council (grant number NE/T000759/1) and the National Research Foundation (CPRR23030680939). We are grateful to the editors and reviewers for their constructive feedback, which improved the manuscript.

CONFLICT OF INTEREST STATEMENT

The authors declare that they have no known financial or non-financial competing interests that could have directly or indirectly influenced the work reported in this paper.

DATA AVAILABILITY STATEMENT

Data were deposited in the Dryad Digital Repository: https://doi.org/10.5061/dryad.pc866t238 (Singini et al., 2025).

STATEMENT ON INCLUSION

This study was conducted in South Africa and includes contributions from both locally based researchers and an international collaborators. Three of the four authors (Edith J. Singini, Brad S. Ripley and Sally Archibald) are based in South Africa, ensuring that local ecological context and perspectives were integrated throughout the research process. All authors were involved from the early stages of study design and analysis. Where appropriate, we cited relevant literature from the region to acknowledge and build on existing local scientific contributions.

ORCID

Edith J. Singini https://orcid.org/0000-0002-6077-6623
Sally Archibald https://orcid.org/0000-0003-2786-3976
Colin P. Osborne https://orcid.org/0000-0002-7423-3718
Brad S. Ripley https://orcid.org/0000-0002-4546-2618

REFERENCES

Aranjuelo, I., Pérez, P., Hernández, L., Irigoyen, J. J., Zita, G., Martínez-Carrasco, R., & Sánchez-Díaz, M. (2005). The response of nodulated alfalfa to water supply, temperature and elevated CO_2 photosynthetic downregulation. *Physiologia Plantarum*, *123*(3), 348–358. https://doi.org/10.1111/j.1399-3054.2005.00459.x

Bates, D., Machler, M., Bolker, B., & Walker, S., C. (2015). Fitting linear mixed effects models using lme4. *Journal of Statistical Software*, *67*, 1–48. https://doi.org/10.18637/jss.v067.i01

Bellasio, C., Quirk, J., Ubierna, N., & Beerling, D. J. (2021). Physiological responses to low CO_2 over prolonged drought as primers for forest-grassland transitions. *Nature Plants*, *8*(9), 1014. https://doi.org/10.1038/s41477-022-01217-8

Bond, W. J. (2008). What limits trees in C_4 grasslands and savannas? *Annual Review of Ecology, Evolution, and Systematics*, *39*, 641–659. https://doi.org/10.1146/annurev.ecolsys.39.110707.173411

Bond, W. J., & Midgley, G. F. (2000). A proposed CO_2-controlled mechanism of woody plant invasion in grasslands and savannas. *Global Change Biology*, *6*(8), 865–869. https://doi.org/10.1046/j.1365-2486.2000.00365.x

Bond, W. J., & Midgley, G. F. (2012). Carbon dioxide and the uneasy interactions of trees and savannah grasses. *Philosophical Transactions of the Royal Society, B: Biological Sciences*, *367*(1588), 601–612. https://doi.org/10.1098/rstb.2011.0182

Bora, Z., Wang, Y. D., Xu, X. W., Angassa, A., & You, Y. (2021). Effects comparison of co-occurring *Vachellia* tree species on understory herbaceous vegetation biomass and soil nutrient: Case of semi-arid savanna grasslands in Southern Ethiopia. *Journal of Arid Environments*, *190*, 104527. https://doi.org/10.1016/j.jaridenv.2021.104527

Bota, J., Medrano, H., & Flexas, J. (2004). Is photosynthesis limited by decreased Rubisco activity and RuBP content under progressive water stress? *New Phytologist*, *162*(3), 671–681. https://doi.org/10.1111/j.1469-8137.2004.01056.x

Buitenwerf, R., Bond, W. J., Stevens, N., & Trollope, W. S. W. (2012). Increased tree densities in South African savannas: >50 years of data suggests CO_2 as a driver. *Global Change Biology*, *18*(2), 675–684. https://doi.org/10.1111/j.1365-2486.2011.02561.x

Campany, C. E., Medlyn, B. E., & Duursma, R. A. (2017). Reduced growth due to belowground sink limitation is not fully explained by reduced photosynthesis. *Tree Physiology*, *37*(8), 1042–1054. https://doi.org/10.1093/treephys/tpx038

Case, M. F., Wigley, B. J., Wigley-Coetsee, C., & Staver, A. C. (2020). Could drought constrain woody encroachers in savannas? *African Journal of Range & Forage Science*, *37*(1), 19–29. https://doi.org/10.2989/10220119.2019.1697363

Criado, M. G., Myers-Smith, I. H., Bjorkman, A. D., Lehmann, C. E. R., & Stevens, N. (2020). Woody plant encroachment intensifies under climate change across tundra and savanna biomes. *Global Ecology and Biogeography*, *29*(5), 925–943. https://doi.org/10.1111/geb.13072

Demmig-Adams, B., Stewart, J. J., & Adams, W. W. (2017). Environmental regulation of intrinsic photosynthetic capacity: An integrated view. *Current Opinion in Plant Biology*, *37*, 34–41. https://doi.org/10.1016/j.pbi.2017.03.008

Drake, J. E., Gallet-Budynek, A., Hofmockel, K. S., Bernhardt, E. S., Billings, S. A., Jackson, R. B., Johnsen, K. S., Lichter, J., McCarthy, H. R., McCormack, M. L., Moore, D. J. P., Oren, R., Palmroth, S., Phillips, R. P., Pippen, J. S., Pritchard, S. G., Treseder, K. K., Schlesinger, W. H., DeLucia, E. J., & Finzi, A. C. (2011). Increases in the flux of carbon belowground stimulate nitrogen uptake and sustain the long-term enhancement of forest productivity under elevated CO_2. *Ecology Letters*, *14*, 349–357. https://doi.org/10.1111/j.1461-0248.2011.01593.x

Duursma, R. A. (2015). Plantecophys—An R package for Analysing and modelling Leaf gas exchange data. *PLoS One*, *10*(11), e0143346. https://doi.org/10.1371/journal.pone.0143346

Farquhar, G. D., & Sharkey, T. D. (1982). Stomatal conductance and photosynthesis. *Annual Review of Plant Physiology and Plant Molecular Biology*, *33*, 317–345. https://doi.org/10.1146/annurev.pp.33.060182.001533

Flexas, J., Bota, J., Cifre, J., Escalona, J. M., Galmés, J., Gulías, J., Lefi, E. K., Martínez-Cañellas, S. F., Moreno, M. T., Ribas-Carbó, M., Riera, D., Sampol, B., & Medrano, H. (2004). Understanding down-regulation of photosynthesis under water stress: Future prospects

13652435, 0, Downloaded from https://besjournals.onlinelibrary.wiley.com/doi/10.1111/1365-2435.70201 by UNIVERSITY OF SHEFFIELD, Wiley Online Library on [28/10/2025]. See the Terms and Conditions (https://onlinelibrary.wiley.com/terms-and-conditions) on Wiley Online Library for rules of use; OA articles are governed by the applicable Creative Commons License

and searching for physiological tools for irrigation management. *Annals of Applied Biology*, *144*(3), 273–283. https://doi.org/10.1111/j.1744-7348.2004.tb00343.x

Fox, J., & Weisberg, S. (2019). *An R companion to applied regression* (Third ed.). Sage Publications.

Grassi, G., & Magnani, F. (2005). Stomatal, mesophyll conductance and biochemical limitations to photosynthesis as affected by drought and leaf ontogeny in ash and oak trees. *Plant, Cell and Environment*, *28*, 834–849. https://doi.org/10.1111/j.1365-3040.2005.01333.x

Higgins, S. I., Bond, W. J., & Trollope, W. S. W. (2000). Fire, resprouting and variability: A recipe for grass-tree coexistence in savanna. *Journal of Ecology*, *88*, 213–229. https://doi.org/10.1046/j.1365-2745.2000.00435.x

Higgins, S. I., & Scheiter, S. (2012). Atmospheric CO_2 forces abrupt vegetation shifts locally, but not globally. *Nature*, *488*(7410), 209–212. https://doi.org/10.1038/nature11238

Huxman, T. E., Hamerlynck, E. P., Moore, B. D., Smith, S. D., Jordan, D. N., Zitzer, S. F., Nowak, R. S., Coleman, J. S., & Seemann, J. R. (1998). Photosynthetic down-regulation in exposed to elevated atmospheric CO_2: Interaction with drought under glasshouse and field (FACE) exposure. *Plant, Cell and Environment*, *21*(11), 1153–1161. https://doi.org/10.1046/j.1365-3040.1998.00379.x

IPCC. (2021). Climate change 2021: The physical science basis, 6th report. IPCC sixth assessment report.

Jiang, M., Medlyn, B. E., Drake, J. E., Duursma, R. A., Anderson, I. C., Barton, C. V. M., Boer, M. M., Carrillo, Y., Castañeda-Gómez, L., Collins, L., Crous, K. Y., De Kauwe, M. G., dos Santos, B. M., Emmerson, K. M., Facey, S. L., Gherlenda, A. N., Gimeno, T. E., Hasegawa, S., Johnson, S. N., … Ellsworth, D. S. (2020). The fate of carbon in a mature forest under carbon dioxide enrichment. *Nature*, *580*, 227–245. https://doi.org/10.1038/s41586-020-2128-9

Kellner, K., Fouché, J., Tongway, D., Boneschans, R., van Coller, H., & van Staden, N. (2022). Landscape function analysis: Responses to bush encroachment in a semi-arid savanna in the Molopo region, South Africa. *Sustainability*, *14*(14), 8616. https://doi.org/10.3390/su14148616

Kirschbaum, M. U. F. (2011). Does enhanced photosynthesis enhance growth? Lessons learned from CO_2 enrichment studies. *Plant Physiology*, *155*(1), 117–124. https://doi.org/10.1104/pp.110.166819

Kohzuma, K., Cruz, J. A., Akashi, K., Hoshiyasu, S., Munekage, Y. N., Yokota, A., & Kramer, D. M. (2009). The long-term responses of the photosynthetic proton circuit to drought. *Plant, Cell and Environment*, *32*(3), 209–219. https://doi.org/10.1111/j.1365-3040.2008.01912.x

Kyalangalilwa, B., Boatwright, J. S., Daru, B. H., Maurin, O., & van der Bank, M. (2013). Phylogenetic position and revised classification of Acacia sl (Fabaceae: Mimosoideae) in Africa, including new combinations in *Vachellia* and *Senegalia*. *Botanical Journal of the Linnean Society*, *172*(4), 500–523. https://doi.org/10.1111/boj.12047

Lenth, R. (2020). *emmeans: Estimated marginal means, aka least-squares means*. R package version 1.8.5. cran.r-project.org/web/packages/emmeans/emmeans.pdf

Lewis, J. R., Verboom, G. A., & February, E. C. (2021). Coexistence and bush encroachment in African savannas: The role of the regeneration niche. *Functional Ecology*, *35*(3), 764–773. https://doi.org/10.1111/1365-2435.13759

Li, W., Hartmann, H., Adams, H. D., Zhang, H., Jin, C., Zhao, C., Guan, D., Wang, A., Yuan, F., & Wu, J. (2018). The sweet side of global change dynamic responses of non-structural carbohydrates to drought, elevated CO_2 and nitrogen fertilization in tree species. *Tree Physiology*, *38*, 1706–1723. https://doi.org/10.1093/treephys/tpy059

Luo, Y., Su, B., Currie, W. S., Dukes, J. S., Finzi, A., Hartwig, U., Hungate, B., McMurtrie, R. E., Oren, R., Parton, W. J., Pataki, D. E., Shaw, M. R., Zak, D. R., & Field, C. B. (2004). Progressive nitrogen limitation of ecosystem responses to rising atmospheric carbon dioxide. *BioScience*, *54*, 731–739. https://doi.org/10.1641/0006-3568

Major, J. E., Mosseler, A., & Malcolm, J. W. (2022). Assimilation efficiencies and gas exchange responses of four species in elevated CO_2 under soil moisture stress and fertilization treatments. *Forests*, *13*(5), 776. https://doi.org/10.3390/f13050776

McDowell, N., Pockman, W. T., Allen, C. D., Breshears, D. D., Cobb, N., Kolb, T., Plaut, J., Sperry, J., West, A., Williams, D. G., & Yepez, E. A. (2008). Mechanisms of plant survival and mortality during drought: Why do some plants survive while others succumb to drought? *New Phytologist*, *178*(4), 719–739. https://doi.org/10.1111/j.1469-8137.2008.02436.x

Medrano, H., Escalona, J. M., Bota, J., Gulías, J., & Flexas, J. (2002). Regulation of photosynthesis of C_3 plants in response to progressive drought:: Stomatal conductance as a reference parameter. *Annals of Botany*, *89*, 895–905. https://doi.org/10.1093/aob/mcf079

O'Connor, T. G., Puttick, J. R., & Hoffman, M. T. (2014). Bush encroachment in southern Africa: Changes and causes. *African Journal of Range & Forage Science*, *31*(2), 67–88. https://doi.org/10.2989/10220119.2014.939996

Quirk, J., Bellasio, C., Johnson, D. A., & Beerling, D. J. (2019). Response of photosynthesis, growth and water relations of a savannah-adapted tree and grass grown across high to low CO_2. *Annals of Botany*, *124*(1), 77–89. https://doi.org/10.1093/aob/mcz048

R Core Team. (2024). *R: A language and environment for statistical computing. Version 4.4. 2*. R Foundation for Statistical Computing.

Ratnam, J., Bond, W. J., Fensham, R. J., Hoffmann, W. A., Archibald, S., Lehmann, C. E. R., Anderson, M. T., Higgins, S. I., & Sankaran, M. (2011). When is a 'forest' a savanna, and why does it matter? *Global Ecology and Biogeography*, *20*, 653–660. https://doi.org/10.1111/j.1466-8238.2010.00634.x

Raubenheimer, S. L., & Ripley, B. S. (2022). CO_2-stimulation of savanna tree seedling growth depends on interactions with local drivers. *Journal of Ecology*, *110*(5), 1090–1101. https://doi.org/10.1111/1365-2745.13863

Ripley, B. S., Raubenheimer, S. L., Perumal, L., Anderson, M., Mostert, E., Kgope, B. S., Midgley, G. F., & Simpson, K. J. (2022). CO_2-fertilisation enhances resilience to browsing in the recruitment phase of an encroaching savanna tree. *Functional Ecology*, *36*(12), 3223–3233. https://doi.org/10.1111/1365-2435.14215

Rugemalila, D. M., Morrison, T., Anderson, T. M., & Holdo, R. M. (2017). Seed production, infestation, and viability in *Acacia tortilis* (synonym: *Vachellia tortilis*) and *Acacia robusta* (synonym: *Vachellia robusta*) across the Serengeti rainfall gradient. *Plant Ecology*, *218*(8), 909–922. https://doi.org/10.1007/s11258-017-0739-5

Ruiz-Vera, U. M., De Souza, A. P., Long, S. P., & Ort, D. R. (2017). The role of sink strength and nitrogen availability in the Down-regulation of photosynthetic capacity in field-grown *Nicotiana tabacum* L. at elevated CO_2 concentration. *Frontiers in Plant Science*, *8*, 998. https://doi.org/10.3389/fpls.2017.00998

Sala, A., Woodruff, D. R., & Meinzer, F. C. (2012). Carbon dynamics in trees: Feast or famine? *Tree Physiology*, *32*(6), 764–775. https://doi.org/10.1093/treephys/tpr143

Scheiter, S., & Higgins, S. I. (2009). Impacts of climate change on the vegetation of Africa: An adaptive dynamic vegetation modelling approach. *Global Change Biology*, *15*(9), 2224–2246. https://doi.org/10.1111/j.1365-2486.2008.01838.x

Scholes, R. J., & Archer, S. R. (1997). Tree-grass interactions in savannas. *Annual Review of Ecology and Systematics*, *28*, 517–544. https://doi.org/10.1146/annurev.ecolsys.28.1.517

Singini, E. J., Archibald, S., Osborne, C. P., & Ripley, S. (2025). Data from: Savanna tree species show contrasting acclimation responses to elevated atmospheric CO_2 concentration and drought. *Dryad Digital Repository*, https://doi.org/10.5061/dryad.pc866t238

13652435, 0, Downloaded from https://besjournals.onlinelibrary.wiley.com/doi/10.1111/1365-2435.70201 by UNIVERSITY OF SHEFFIELD, Wiley Online Library on [28/10/2025]. See the Terms and Conditions (https://onlinelibrary.wiley.com/terms-and-conditions) on Wiley Online Library for rules of use; OA articles are governed by the applicable Creative Commons License

Skowno, A. L., Thompson, M. W., Hiestermann, J., Ripley, B., West, A. G., & Bond, W. J. (2017). Woodland expansion in south African grassy biomes based on satellite observations (1990–2013): General patterns and potential drivers. *Global Change Biology*, *23*(6), 2358–2369. https://doi.org/10.1111/gcb.13529

Staver, A. C., Archibald, S., & Levin, S. A. (2011). The global extent and determinants of savanna and forest as alternative biome states. *Science*, *334*(6053), 230–232. https://doi.org/10.1126/science.1210465

Stevens, N., Lehmann, C. E. R., Murphy, B. P., & Durigan, G. (2017). Savanna woody encroachment is widespread across three continents. *Global Change Biology*, *23*(1), 235–244. https://doi.org/10.1111/gcb.13409

Strauss, M. K., & Packer, C. (2015). Did elephant and giraffe mediate in the prevalence of palatable species in an East African acacia woodland? *Journal of Tropical Ecology*, *31*(1), 11–12. https://doi.org/10.1017/S0266467414000625

Telford, E. M., Stevens, N., Midgley, G. F., & Lehmann, C. E. R. (2023). Nodulation alleviates the stress of lower water availability in *Vachellia sieberiana*. *Plant Ecology*, *224*(4), 387–402. https://doi.org/10.1007/s11258-023-01302-8

Vu, J. C. V., Allen, L. H., & Gesch, R. W. (2006). Up-regulation of photosynthesis and sucrose metabolism enzymes in young expanding leaves of sugarcane under elevated growth CO_2. *Plant Science*, *171*(1), 123–131. https://doi.org/10.1016/j.plantsci.2006.03.003

Walters, M. B., & Reich, P. B. (2000). Seed size, nitrogen supply, and growth rate affect tree seedling survival in deep shade. *Ecology*, *81*(7), 1887–1901. https://doi.org/10.1890/0012-9658(2000)081[1887:SSNSAG]2.0.CO;2

Wigley, B. J., Bond, W. J., & Hoffman, M. T. (2010). Thicket expansion in a South African savanna under divergent land use: Local vs. global drivers? *Global Change Biology*, *16*(3), 964–976. https://doi.org/10.1111/j.1365-2486.2009.02030.x

Wigley, B. J., Cramer, M. D., & Bond, W. J. (2009). Sapling survival in a frequently burnt savanna: Mobilisation of carbon reserves in *Acacia karroo*. *Plant Ecology*, *203*(1), 1–11. https://doi.org/10.1007/s11258-008-9495-x

Zheng, Y. P., Li, F., Hao, L. H., Yu, J. J., Guo, L. L., Zhou, H. R., Ma, C., Zhang, X. X., & Xu, M. (2019). Elevated CO_2 concentration induces photosynthetic down-regulation with changes in leaf structure, non-structural carbohydrates and nitrogen content of soybean. *BMC Plant Biology*, *19*, 255. https://doi.org/10.1186/s12870-019-1788-9

Zotz, G., Pepin, S., & Körner, C. (2005). No down-regulation of leaf photosynthesis in mature forest trees after three years of exposure to elevated CO_2. *Plant Biology*, *7*(4), 369–374. https://doi.org/10.1055/s-2005-837635

SUPPORTING INFORMATION

Additional supporting information can be found online in the Supporting Information section at the end of this article.

Figure S1: Experimental design and setup. (A) Schematic representation of the factorial design combining two CO_2 treatments (ambient: 400 ppm; elevated: 550 ppm) with two water regimes (well watered and droughted). (B) Photograph of the experimental setup inside the open-top chamber facility (Rhodes University Elevated CO_2 Facility), showing potted seedlings under treatment conditions. Grass species were also included in the full experiment, but are not presented in this study.

Figure S2: Average soil volumetric water content (%) across 1 year (2022) in pots exposed to ambient and elevated CO_2 concentrations. Points represent means ± SD ($n = 16$ sensors per treatment).

Figure S3: Stomatal limitation (SL) under droughted and well-watered conditions, and relative stomatal (RSL) and relative metabolic limitations (RML) across five savanna tree species (*Vachellia tortilis*, *V. sieberiana*, *V. karroo*, *V. robusta* and *Senegalia burkei*) grown under ambient (400 ppm) and elevated (550 ppm) CO_2. SL under drought and SL under well-watered conditions represent the percentage reduction in photosynthesis resulting from stomatal closure under their respective water treatments. RSL and RML were calculated following Ripley et al. (2007) to quantify the proportional contribution of stomatal and metabolic processes to photosynthetic limitation under drought. Error bars indicate ± standard error of the mean ($n = 6$).

Figure S4: Geographic distribution of *Vachellia tortilis*, *V. sieberiana* and *V. karroo* (known encroaching species), and *V. robusta* and *Senegalia burkei* (non-encroaching species) across Africa. Species occurrence points represent GPS coordinates obtained from the Global Biodiversity Information Facility (GBIF), and only terrestrial records within the African continent are shown.

Table S1: Results from mixed effects models testing the effects of volumetric soil water content (VWC) and CO_2 concentration, as well as their interaction, on photosynthetic rate (*A*), maximum carboxylation rate (*V*cmax), maximum electron transport rate (*J*max), stomatal conductance (g_{ST}), intercellular CO_2 (Ci) and above-ground growth rate (GR) in *Vachellia karroo*, *V. sieberiana*, *V. tortilis*, *V. robusta* and *Senegalia burkei*. Interaction terms were initially included in all models and were then removed when results were non-significant. The models were then re-run without the interaction term.

Table S2: Encroachment status, supporting growth traits and literature-based evidence for five savanna tree species evaluated in this study. The encroacher classification is based on documented increases in population density or range expansion, often in response to land-use changes or CO_2 enrichment. Non-encroachers are characterised by stable or declining populations and limited colonisation capacity under similar conditions.

How to cite this article: Singini, E. J., Archibald, S., Osborne, C. P., & Ripley, B. S. (2025). Savanna tree species show contrasting acclimation responses to elevated atmospheric CO_2 concentration and drought. *Functional Ecology*, *00*, 1–12. https://doi.org/10.1111/1365-2435.70201

13652435, 0, Downloaded from https://besjournals.onlinelibrary.wiley.com/doi/10.1111/1365-2435.70201 by UNIVERSITY OF SHEFFIELD, Wiley Online Library on [28/10/2025]. See the Terms and Conditions (https://onlinelibrary.wiley.com/terms-and-conditions) on Wiley Online Library for rules of use; OA articles are governed by the applicable Creative Commons License